LIMNOLOGY and OCEANOGRAPHY

ASLO

Limnol. Oceanogr. 9999, 2020, 1–16

doi: 10.1002/lno.11671

Autonomous vehicle surveys indicate that flow reversals retain juvenile fishes in a highly advective high-latitude ecosystem

Robert M. Levine,[1*] **Alex De Robertis**,[2] **Daniel Grünbaum**,[1] **Rebecca Woodgate**,[1] **Calvin W. Mordy**,[3,4] **Franz Mueter**,[5] **Edward Cokelet**,[4] **Noah Lawrence-Slavas**,[4] **Heather Tabisola**[3,4]

[1]School of Oceanography, University of Washington, Seattle, Washington
[2]Alaska Fisheries Science Center, National Marine Fisheries Service, NOAA, Seattle, Washington
[3]Cooperative Institute for Climate, Ocean, and Ecosystem Studies, University of Washington, Seattle, Washington
[4]Pacific Marine Environmental Laboratory, NOAA, Seattle, Washington
[5]College of Fisheries and Ocean Sciences, University of Alaska Fairbanks, Juneau, Alaska

Abstract

Summer surveys of the Chukchi Sea indicate that high densities of age-0 gadid fishes, historically Arctic cod (*Boreogadus saida*) but recently also walleye pollock (*Gadus chalcogrammus*), dominate the pelagic fish community. Adults are comparatively scarce, suggesting that either overwinter survivorship of age-0 gadids is low, or that they emigrate to other areas of the Pacific Arctic. To examine population movement, we conducted repeat acoustic surveys with saildrone autonomous surface vehicles equipped with echosounders throughout summer 2018. The saildrones' range and endurance enabled two large-scale surveys of the U.S. Chukchi shelf. Acoustic backscatter, a proxy for fish density, was highest in regions with sea surface temperatures of 6–8°C, and lowest in areas influenced by recent ice melt. A subarea of the central Chukchi was surveyed a total of four times; backscatter in this subarea increased by > 85% from late-July to mid-September. As summer progressed, fish developed more extensive diel vertical migrations and backscatter from individuals doubled. Both changes suggest increases in backscatter were driven primarily by increasing body size. Particle tracking simulations indicated age-0 gadids were likely retained over the Chukchi shelf by extended periods of wind-driven southward flow during the survey period before strong northward flow in late fall transported them to the north. These findings suggest that in summer 2018, age-0 gadids were advected northward to the Chukchi shelf from the northern Bering Sea, where they were retained during a period of growth until late fall before being advected farther north toward the Chukchi and Beaufort shelf breaks.

Arctic gadids, particularly Arctic cod (*Boreogadus saida*), dominate the pelagic fish community in the Pacific Arctic ecosystem of the northern Bering, Chukchi, East Siberian, and Beaufort Seas. Arctic cod have a circumarctic distribution and are abundant throughout the shallow shelves of the Arctic marginal seas as well as the Central Arctic Basin (Mecklenburg et al. 2018). Arctic cod are key pelagic secondary consumers that serve as a central trophic link between plankton and higher trophic levels (Bradstreet et al. 1986; Whitehouse and Aydin 2016), supporting large migratory populations of seabirds (Matley et al. 2012) and marine mammals (Bradstreet et al. 1986). The Pacific Arctic is undergoing rapid changes associated with surface warming and loss of sea ice (Steele et al. 2008; Frey et al. 2015; Woodgate 2018). These changes have the potential to negatively impact Arctic cod growth and survival in this region and alter species distributions.

Recent studies suggest that the warming conditions in the Pacific Arctic are becoming increasingly hospitable for more boreal species such as walleye pollock (*Gadus chalcogrammus*) (Laurel et al. 2016; Huntington et al. 2020). Historically, trawl surveys conducted in the Chukchi Sea have found that pelagic biomass is dominated by age-0 (born within the past year) Arctic cod (Quast 1974; Norcross et al. 2010; Logerwell et al. 2015). Acoustic-trawl surveys conducted in 2017 and 2019 indicate that age-0 walleye pollock have become more abundant on the Chukchi shelf (R. M. Levine unpubl.). As the region changes due to increasing temperatures, walleye pollock distributions may expand to the north and become a potentially significant component of the gadid community on the Chukchi shelf.

Little is known about the distribution and movements of pelagic fish populations in the region, particularly in the Chukchi Sea. Acoustic-trawl surveys conducted in summer

*Correspondence: leviner@uw.edu

Additional Supporting Information may be found in the online version of this article.

2012 and 2013 established a baseline of distributions of pelagic fishes in the U.S. northern Bering and Chukchi Seas (De Robertis et al. 2017). These surveys documented large numbers of pelagic age-0 Arctic cod, with the highest abundances in the northern Chukchi Sea where the average length was 3.5 cm and < 0.3% were greater than 6.5 cm (De Robertis et al. 2017). However, this and other surveys in the area indicate that older Arctic cod are comparatively rare on the U.S. Chukchi shelf (Logerwell et al. 2015; De Robertis et al. 2017).

Estimates of the reproductive potential of the Arctic cod population in the survey region indicate that observed densities of adults are likely insufficient to produce the large numbers of age-0 fish observed in the acoustic-trawl surveys (Marsh et al. 2019). It is likely that age-0 Arctic cod observed on the Chukchi shelf in summer are produced by adults that seasonally migrate into the region to spawn, or from eggs and larvae spawned in other areas and subsequently transported into the region. Large-scale horizontal migration of Arctic cod to spawning aggregation sites has been observed in the Barents Sea (Gjøsæter 1995) and Russian Arctic (Ponomarenko 1968). Recent work has hypothesized that a similar pattern of seasonal migration may occur in the Pacific Arctic (Forster et al. 2020). Similarly, walleye pollock have recently become more abundant in the northern Bering Sea (Stevenson and Lauth 2019), and this may have increased the supply of walleye pollock larvae that enter the Chukchi Sea from the south in recent years. The low densities of age-1 + relative to age-0 gadids found on the Chukchi shelf indicate that either overwinter survival of age-0s retained in the area is very low, or that the Chukchi shelf serves only as a summer nursery area, after which age-0s subsequently emigrate or are transported to other areas (De Robertis et al. 2017).

The likelihood of these scenarios is partially constrained by local advective regimes. The Chukchi Sea is a region of seasonally high advection, with strong northward currents that may transport eggs and larvae from the south (Fig. 1). High northward transport across the shelf occurs during the summer and fall (Woodgate et al. 2005; Stabeno et al. 2018), yielding residence times of Pacific Waters in the Chukchi of 4–5 months, although this residence time has likely decreased in recent years (Woodgate et al. 2005; Woodgate 2018). This movement of Pacific water toward the Arctic structures the species composition and distribution of plankton communities in the Chukchi Sea, with many species being transported into the Chukchi Sea from the Bering Sea (Eisner et al. 2013; Ershova et al. 2015; Sigler et al. 2017). Interannual variability in phytoplankton, zooplankton and ichthyoplankton communities is strongly influenced by changes in oceanographic forcing, as indicated by associations between water masses of southern origin and community composition (Norcross et al. 2010; Danielson et al. 2017; Pinchuk and Eisner 2017; Spear et al. 2019).

The reproductive biology of Arctic cod and walleye pollock in the context of the advective regime provides additional clues to the origins of fish observed on the Chukchi shelf.

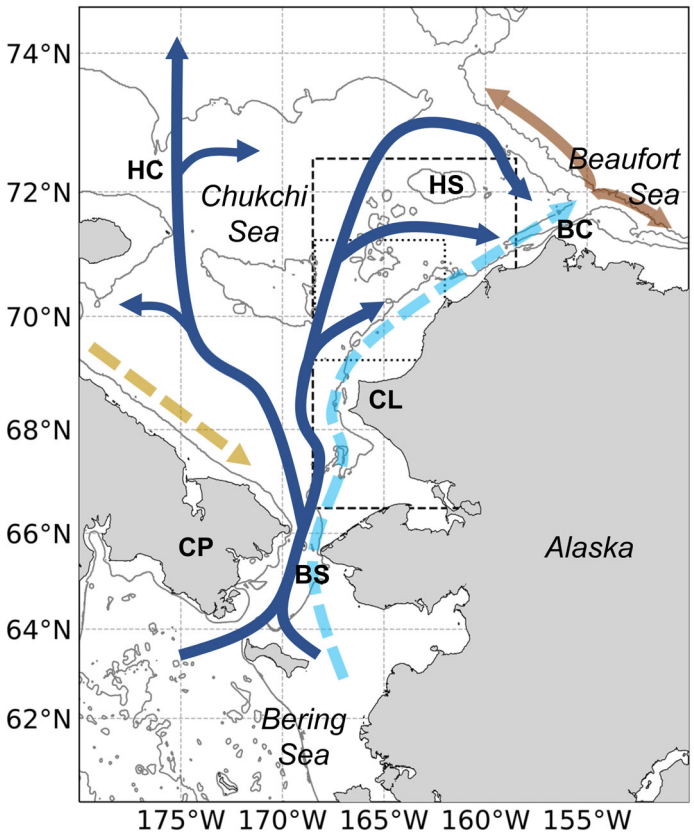

Fig. 1. Map of the study region, showing the primary transport pathways through the Chukchi Sea based on Corlett and Pickart (2017): Alaskan coastal current (light blue), Bering Sea water (dark blue), Siberian coastal current (gold), slope current (brown, westward) and shelf break jet (brown, eastward). Dashed lines indicate seasonal currents. Survey regions are indicated for the large-scale survey (dashed box) and small-scale survey (dotted box). Geographic features referred to in the text are indicated in bold: Bering Strait (BS), Chukotka Peninsula (CP), Cape Lisburne, (CL), Herald Canyon (HC), Hanna Shoal (HS), and Barrow Canyon (BC). The 40-, 100-, and 1000-m depth contours are shown.

Arctic cod are known to spawn in fall and winter under sea ice on the shallow shelves of the Arctic marginal seas (Ponomarenko 2000). Fertilized eggs are buoyant and develop under ice cover at the ice–water interface (Ponomarenko 2000). Pollock similarly produce pelagic eggs and, as larvae, remain close to the surface (Spencer et al. 2020). Development time in both species is temperature dependent, with time to 50% hatching of Arctic cod in laboratory studies ranging from 31 d at 3.8°C to 67 d at –0.4°C and approximately half of that time across these temperatures for walleye pollock (Laurel et al. 2018). Arctic cod hatching has been observed from December through August, with a peak during May/June (Bouchard and Fortier 2011). Ichthyoplankton surveys and otolith aging of larval and juvenile Arctic cod in other regions of the Arctic indicates that spawning occurs over a period of months, producing an extended distribution of larval fish throughout the summer

rather than a single short pulse or a set of discrete pulses (Bouchard and Fortier 2011; Bouchard et al. 2016). The spawning period of walleye pollock in the Bering Sea extends from early winter into early fall, with spawning in the northern Bering shelf highest in early summer (Hinckley 1987).

It is hypothesized that age-0 gadids on the Chukchi shelf are spawned to the south and are advected northward onto the Chukchi shelf in summer. Particle tracking simulations suggest that variations in wind and current patterns drive the interannual variability observed in late-summer distribution in the Chukchi Sea (C. D. Vestfals unpubl.). The age-0 gadids are then advected further to the north in the fall. Observations and modeled transport of larval Arctic cod suggest that spawning occurs at multiple locations in the Pacific Arctic (Vestfals et al. 2019; C. D. Vestfals unpubl.). Three key areas have been proposed as spawning areas for age-0 Arctic cod on the Chukchi shelf: the northern Bering Sea, along the Chukotka Peninsula in western Bering Strait, and the Beaufort Sea (Fig. 1; Kono et al. 2016; Vestfals et al. 2019). Acoustic-trawl abundance estimates in 2012 were lower than those in 2013 which is consistent with the hypothesis that lower annual northward transport in 2012 (e.g., Woodgate 2018) resulted in fewer age-0 Arctic cod originating in the Bering Sea were advected to the northeast Chukchi Sea by the time of the survey (C. D. Vestfals unpubl.). Larval Arctic cod have also been found in the northern Chukchi and western Beaufort Seas, in particular near Barrow Canyon. These fish may have been transported southward via up-canyon advection from aggregations of adult Arctic cod distributed to the north along the Beaufort shelf break (Geoffroy et al. 2011; Parker-Stetter et al. 2011; C. D. Vestfals unpubl.). Although Arctic cod are historically the most abundant species, advective transport is likely the main process driving the presence of all age-0 gadids on the Chukchi shelf. Walleye pollock and saffron cod (*Eleginus gracilis*) are abundant in the northern Bering and southern Chukchi Seas, respectively (De Robertis et al. 2017; Stevenson and Lauth 2019). Eggs and larvae of these species are likely to follow transport pathways similar to Arctic cod on the Chukchi shelf.

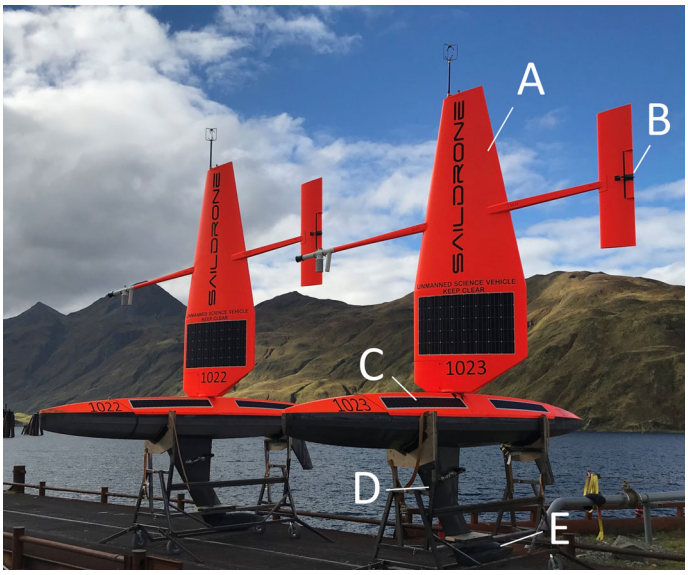

Fig. 2. Saildrone uncrewed surface vehicles upon recovery in Dutch Harbor, Alaska. (**a**) Wing, (**b**) trim tab, (**c**) hull, (**d**) keel, and (**e**) transducer mount. Image courtesy of Saildrone, Inc.

In this study, we sought to test the hypothesis that age-0 gadids in the Chukchi Sea are typically advected north during the summer, and that their distribution would shift northward during the open-water season. We used uncrewed surface vehicles (USVs) to conduct repeat acoustic surveys of the northeastern Chukchi Sea to quantify the intraseasonal variability in the spatial distribution of gadids in summer 2018. By conducting repeat surveys, we aimed to: (1) infer the source location of the age-0 gadid population in the northeastern Chukchi Sea in summer; (2) evaluate what movements of the fish population may reveal about the role of the northeastern Chukchi Sea as a nursery area for age-0 Arctic cod and other gadid fishes; and (3) ascertain whether, when, and how fish were transported out of the study area.

Methods

Survey design and data collection

Two Saildrone generation 5 USVs (SD-1022 and SD-1023, Saildrone, Inc., Fig. 2) were used to conduct an acoustic survey of pelagic sound-scattering organisms on the Chukchi shelf. The vehicles were deployed from Dutch Harbor, Alaska, on 30 June 2018 and recovered in the same location on 06 October (98 d). The saildrone is a 7-m long wind-propelled vehicle which uses an actuator-controlled trim tab to manipulate a 5-m wing sail (Mordy et al. 2017; De Robertis et al. 2019). The vehicle autonomously navigates between operator-specified waypoints, with near real-time navigation, data reporting, and instrument control via satellite link. Onboard instrumentation operates on battery power, which is replenished by solar panels on the hull and wing. From 14 July to 24 September 2018 (72 d) the saildrones conducted acoustic surveys of the U.S. continental shelf region of the Chukchi Sea.

To compare the distribution of backscatter during mid and late summer, two large-scale surveys were completed from 20 July to 16 August and 24 August to 11 September. The surveys were conducted between 66.5°N and 72.5°N and 168.6°W and 159.5°W (Fig. 1, area encompassed by the dashed line) along the 0.5° latitude spaced transects as surveyed by research vessels in 2012 and 2013 (De Robertis et al. 2017). Two additional surveys were conducted on a subset of four of the transect lines between 69.5°N and 71°N from 20 July to 03 August and from 13 August to 28 August. Along with the two large-scale surveys, this resulted in four replicate small-scale surveys in a region of previously (i.e., 2012 and 2013) observed high acoustic backscatter in the northeastern

Chukchi Sea (Fig. 1, area indicated by dotted box). Both large-scale surveys and the additional two small-scale surveys were conducted from north to south along east–west acoustic transects. In total, the two saildrones traveled 7610 nautical miles (14,093 km; hereafter referred to as nmi) in the Chukchi Sea at an average speed of 1.2 m s^{-1}.

To measure backscatter from fishes, each saildrone was outfitted with a Simrad wideband autonomous transceiver (WBAT-mini) split-beam echosounder with a Simrad ES38-18/200-18C transducer (three-channel split-beam 38 kHz and single-beam 200 kHz, both with a half power beamwidth of 18°) gimbal-mounted on the keel at a depth of 1.9 m (see De Robertis et al. 2019 for details on echosounder integration). To manage power consumption, 12-min ping ensembles were transmitted between one and five times per hour (90% of data were collected with the instrument pinging continuously) defined by the operator depending on the battery state. Each ensemble consisted of simultaneous 38 and 200 kHz narrowband pings every 1.5 s using a 0.5-ms pulse duration. Backscatter was recorded to 75 or 150 m range depending on the bottom depth. Electrical interference from the vehicle's systems precluded the use of the 200 kHz data (this issue has since been resolved by Saildrone). The echosounders were calibrated after deployment using a 60-mm copper sphere for the 38-kHz transducer following the standard sphere method (Demer et al. 2015).

Sensors aboard the saildrone monitored environmental conditions throughout the deployment at 1-min intervals (for a full suite of sensors, see Mordy et al. 2017). Water temperature and salinity at 0.5 m depth were measured using a pair of conductivity, temperature, and depth (CTD) sensors (Saildrone[3], RBR Ltd. and Sea-Bird SBE-37) on each USV. In situ comparisons between calibrated sensor pairs agreed to temperatures within ~ 0.01°C and salinities to within ~ 0.02 (PSS-78). Photosynthetically active radiation was measured at 2.5 m above the sea surface (LI-192SA, LI-COR, Inc.), and wind speed was measured using an anemometer mounted on the wing at 5.2 m (1590-PK-020, Gill Instruments Ltd.).

Inferring the identity of acoustic targets

In acoustic-trawl surveys, backscatter is attributed to species based on direct sampling (e.g., trawling) of acoustic scatterers, and by applying knowledge of the abundance and behavior (e.g., schooling characteristics and depth distributions) of the species in the study area (Horne 2000). We were unable to conduct any trawl sampling in 2018, and thus had to rely on observations from other years to interpret the acoustic observations. Surveys in 2012 and 2013 found the age-0 Arctic cod population in the Chukchi Sea to be > 35 times larger than any other observed species (De Robertis et al. 2017). Preliminary results from pelagic trawls conducted in 2017 and 2019 also indicate that most of the acoustic scattering at 38 kHz in this area is attributable to age-0 gadids. However, walleye pollock have become more abundant in recent years. Age-0 gadids made up > 95% of the trawl catch per unit effort in 2017 (85% Arctic cod and 10% walleye pollock by number) and > 85% of the catch per unit effort in 2019 (45% Arctic cod and 40% walleye pollock; R. M. Levine and S. Wildes unpubl.). As in previous years (De Robertis et al. 2017), other gadids such as saffron cod and Pacific cod (*Gadus macrocephalus*), and other strong sound scattering pelagic fishes such as capelin (*Mallotus villosus*) and Pacific herring (*Clupea pallasii*), were present in comparatively low abundance in 2017 and 2019 (R. M. Levine unpubl.) and occupied only a small portion of the Chukchi shelf. Although trawl sampling was not conducted during 2018, these surveys from previous and subsequent years strongly suggest that age-0 Arctic cod and walleye pollock likely dominated acoustic backscatter. Therefore, our analysis assumed that the acoustic-based measures of fish density collected by the saildrones primarily reflect the abundance and distribution of age-0 Arctic cod and walleye pollock.

Acoustic data processing

Acoustic data were processed using Echoview 10.0 (Echoview Software Pty Ltd). Mean volume backscattering strength (S_v, dB re 1 m^{-1}) at 38 kHz was used as a proxy for fish abundance. Sound speed and absorption were determined from 128 CTD casts collected during a 2017 survey of the U.S. continental shelf region of the Chukchi Sea between 67°N and 72.5°N. A mean sound speed of 1466.3 m s^{-1} was used for acoustic data post-processing, comparable to estimates of mean sound speed of the same region in other years (1470 m s^{-1} in 2013, 1472 m s^{-1} in 2019). Estimates fish backscatter were not sensitive to the sound speed used: if sound speed from any individual cast (range of 1454.6–1484.4 m s^{-1}) was used for the analysis instead of the mean value, backscatter changed by < 1%. In previous acoustic surveys, 38-kHz backscatter was dominated by backscatter with a frequency response consistent with that of fish (~ 96% in 2012 and 2013, De Robertis et al. 2017). During periods of elevated sea state, bubble entrainment caused attenuation of the transmitted signal. These pings were removed following the methods in De Robertis et al. (2019). The nautical area scattering coefficient (s_A, m^2 nmi^{-2}) was integrated from 4 m below the sea surface to 0.5 m above the sounder-detected seafloor (as determined by Echoview's "best bottom candidate" algorithm and manually corrected after visual inspection where necessary) using a −70 dB re 1 m^{-1} threshold in 0.1 nmi along-track and 5-m vertical bins. s_A is a proxy for fish abundance: it is proportional to fish density if the proportion of incident signal backscattered from the average fish in the population remains constant (MacLennan et al. 2002).

To compare backscatter between repeat surveys, the survey area was gridded into 0.5° latitude by 0.5° longitude cells. For large-scale surveys, only grid cells that contained data from both surveys were included (Fig. 3), resulting in 75 valid grid cells encompassing 993 and 805 nmi of acoustic observations

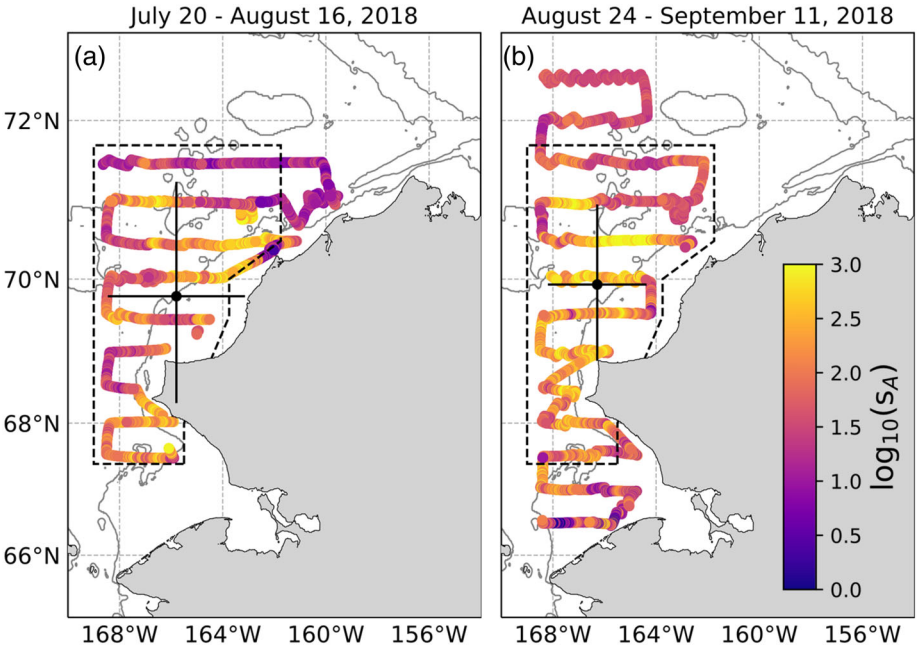

Fig. 3. 38-kHz backscatter (s_A, m^2 nmi^{-2}) along the saildrone trackline during the (**a**) first and (**b**) second large-scale surveys. Center of gravity and variance of spatial distribution computed from the gridded cells common to both surveys (region encompassed by the dashed line) are indicated by the black circles and lines, respectively. The 40-, 100-, and 1000-m depth contours are shown.

from the first and second surveys, respectively. Mean s_A was computed from acoustic measurements within each grid cell. The overall mean s_A and the standard errors for all valid grid cells were estimated for each survey by fitting a geostatistical model to the gridded data with a separate mean by survey and constant spatial autocorrelation across surveys. The model was fitted via generalized least squares (GLS) using a Gaussian spatial correlation structure with a nugget effect (Wackernagel 2013). The same gridding and GLS model structure were applied to the four small-scale surveys to calculate mean backscatter and identify variability over time. In each of the four small-scale surveys, a subset of 42 grid cells containing 350 nmi of overlapping trackline was used for analysis (Fig. 5). The mean location of the distribution weighted by mean s_A (center of gravity, Eq. 1 in Woillez et al. 2007), and the mean square distance between a measurement and the center of gravity (variance of spatial distribution, Eq. 3 in Woillez et al. 2007), were used to describe changes in the spatial distribution of the backscatter.

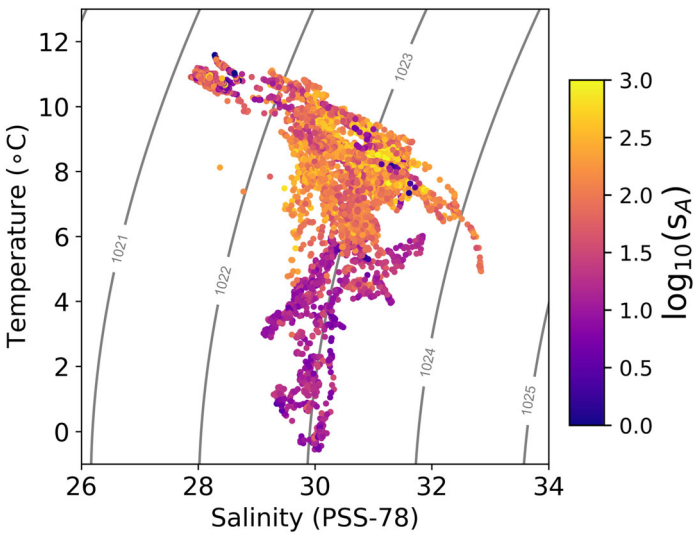

Fig. 4. Ten-minute averaged temperature and salinity at 0.5 m depth measured by sensors on the keel of the saildrone during the large-scale surveys (Fig. 3). Color of points indicates depth-integrated water column 38-kHz backscatter (s_A, m^2 nmi^{-2}). Contours indicate potential density.

Measurements of backscattering cross-section (σ_{bs}, m^2) of individual scatterers during the four small-scale surveys were calculated from single targets identified with Echoview's split-beam single target detection (method 2) algorithm. To minimize potential biases introduced by multiple overlapping targets being interpreted as a single fish, single target detection was limited to areas where density was low. The estimated number of animals per reverberation volume (Nv, Sawada et al. 1993) was determined in 100 ping along-track and 5-m vertical bins based on a target strength (TS, dB re 1 m^2; $TS = 10 \log_{10}(\sigma_{bs})$, where σ_{bs} is the backscattering cross-section, see MacLennan et al. 2002). Based on previous catch results indicating that Arctic cod were likely the dominant scatterer, Nv was calculated using a TS of −57.3 dB re 1 m^2 which assumes a mean Arctic cod size of 3.5 cm (De Robertis

et al. 2017) and is similarly appropriate for walleye pollock of the same size class (Table S1). Single targets in grid cells where Nv > 0.04 were excluded from further analyses, as recommended by Sawada et al. (1993).

To investigate changes in acoustic strength of targets during the small-scale surveys, the mean σ_{bs} of all targets during each day of each small-scale survey was calculated (79–21,542 targets per day, median of 2893 targets). The daily means were used to model the changes in σ_{bs} as a linear function of time (yearday). A TS-length relationship developed primarily from age-0 Arctic cod (Geoffroy et al. 2016) was used to infer fish length at the midpoint of each small-scale survey from σ_{bs}, defined as

$$SL = 10^{\left(\frac{10\log_{10}(\sigma_{bs})+65.13}{14.33}\right)}, \quad (1)$$

where SL is standard length (*see* Table S1 for additional details). Fish density (fish m^{-2}) at the midpoint of each small-scale survey was calculated using model-predicted σ_{bs} following MacLennan et al. (2002).

Vertical distributions of age-0 Arctic cod were quantified by calculating the weighted mean depth of the backscatter from the entire water column in 1-h intervals (Eq. 2 in Woillez et al. 2007). Hourly measurements were classified as day or night based on photosynthetically active radiation measurements from the saildrones' sensors, using a day/night threshold value of photosynthetically active radiation of 10 μmol photons s^{-1} m^{-2}, with 26% of the survey measurements occurring at night. To investigate linear trends in weighted mean depth over the duration of the surveys, an analysis of covariance was used to model the weighted mean depth of backscatter as a linear function of time (yearday), allowing the intercept and slope to differ between day and night. The model was fit via GLS to account for possible temporal autocorrelation, assuming a continuous first-order autoregressive time series structure (corAR1, Pinheiro et al. 2019).

Particle tracking simulations

The potential for physical retention of fishes in the northeastern Chukchi Sea was examined using calculations completed using the OceanParcels python library (Lange and van Sebille 2017) which simulates the advection of passive particles from results of a numerical ocean model. Particles were tracked using a 1/12° resolution 3D velocity field obtained from the hybrid coordinate ocean model (HYCOM) global analysis output (https://hycom.org), at 3-h time resolution from 20 July to 18 September 2018. This model has 40 depth levels, with 5-m intervals from 10 to 50 m depth. HYCOM uses the Navy Coupled Ocean Data Assimilation system which assimilates satellite altimeter and sea surface temperature data, and in situ temperature and salinity profiles from ship, drifter, and mooring instrumentation. Surface forcing for the HYCOM run is taken from the Navy Global Environmental Model (Hogan et al. 2014). The particles were seeded in areas where the first large-scale survey suggested (from observed grid cell mean s_A and survey-wide mean σ_{bs}) that fish were abundant. A single particle was seeded at the center of each model grid cell where observed fish density was ≥ 0.1 fish m^{-2} (96 of 98 model grid cells) on the start date of the first large-scale survey (20 July).

Particle positions were calculated at 3-h intervals. To evaluate the potential for depth-dependent variability in transport, four separate model runs were conducted seeding particles at fixed depths of either 10, 20, 30, or 40 m. This range of depths encompasses the portion of the water column where most of the fish were located (> 85% of backscatter was observed from 10 to 40 m). To evaluate retention in the northeastern Chukchi Sea, we identified the proportion of particles at each time step that were (1) contained within the small-scale survey region or (2) found in the Beaufort Sea or on the Chukchi Sea slope (> 100 m bottom depth).

Results

Repeat large-scale surveys

The saildrones successfully completed two large-scale surveys of the U.S. continental shelf of the Chukchi Sea (Fig. 3). Sea-ice north of 71.5°N limited the northern extent of the first survey which was completed from 20 July to 16 August 2018 by a single saildrone. The second survey was completed from 24 August to 11 September 2018 by tasking two saildrones independently with the northern and southern portions of the survey.

Although the mean backscatter in the large-scale survey area increased slightly from a mean s_A of 144 (± 37 SE) m^2 nmi^{-2} during the first survey to 188 (± 50 SE) m^2 nmi^{-2} during the second survey, the means were not significantly different (GLS, *t*-test $p = 0.37$). Fish distributions were similar in both surveys, suggesting there was no large-scale net advection of the population through the area during the survey period. The center of gravity of the backscatter shifted 18.7 km west (−165.79°W to −166.28°W) and 17.4 km north (from 69.77°N to 69.92°N), while exhibiting a slight decrease in variance of spatial distribution (−0.44° and −0.75° in latitude and longitude, respectively; Fig. 3). During both surveys > 50% of the total backscatter occurred between 70°N and 71°N.

Temperature and salinity at 0.5 m depth ranged from −0.7°C to 11.4°C and from 26.5 to 32.8 psu during the large-scale surveys (Fig. 4). The coldest water was encountered north of 71°N, where surface conditions suggested recent mixing with sea ice meltwater (< 7°C and salinity < 30 psu). In areas where meltwater was present at the surface, backscatter was low; 92.9% of backscatter was observed in areas where the surface temperature was greater than 6°C and salinity was greater than 29 psu (Figs. 4, S1).

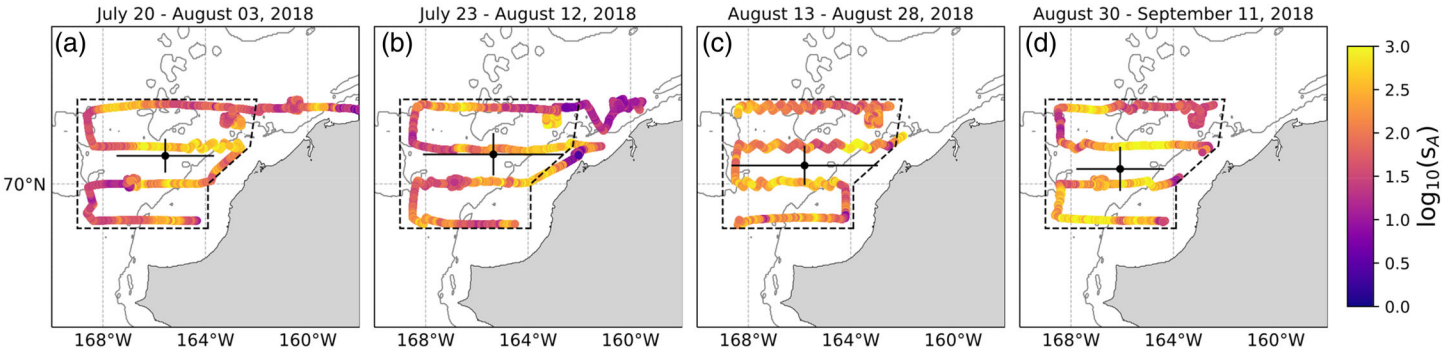

Fig. 5. 38-kHz backscatter (s_A, m^2 nmi^{-2}) along the saildrone trackline during the (**a**) 1st, (**b**) 2nd, (**c**) 3rd, and (**d**) 4th small-scale surveys. The center of gravity and variance of the spatial distribution computed from the gridded cells common to all surveys (region encompassed by the dashed line) is indicated by the black circles and lines, respectively. Note that the first two survey periods overlap in time. The 40- and 100-m depth contours are shown.

Repeat small-scale surveys

The small-scale surveys (four-transect subarea of the large-scale survey from 69.5°N to 71°N) lasted 12–21 d: 20 July–03 August, 23 July–12 August, 13–28 August (including a 5-d gap in sampling from 17 to 21 August), and 30 August to 11 September (Fig. 5). Mean backscatter within the 42 grid cells of the small-scale survey area varied among surveys, increasing from 197 (± 53 SE) to 369 (± 80 SE) m^2 nmi^{-2} over the course of the summer (GLS, *t*-test p = 0.03, Table 1). The distribution of the population within the small-scale survey region did not shift appreciably among surveys. The center of gravity shifted slightly to the southwest between the first and last survey (19.4 km to the south and 19.3 km to the west, from −165.56°W 70.37°N to −166.08°W 70.19°N, Fig. 5).

The vertical distribution of fish during the small-scale surveys was consistent with the onset of vertical migration behavior. As the summer progressed, the weighted mean depth of backscatter remained shallow at night, but daytime depth increased after the second survey (Fig. 6a–d). Weighted mean depth during daylight hours increased from 17.7 (± 0.2 SE) to 30.0 (± 0.4 SE) m over the period of 53 d between the 1st and 4th survey (Fig. 6a–d). In contrast, weighted mean depth at night showed less variation, ranging from 16.6 (± 0.5 SE) to 19.6 (± 0.5 SE) m during the four surveys. Daylight hours decreased from 24 h per day at the start of the 1st survey to 14 h per day at the end of the 4th survey. Weighted mean depth differed between day and night (significant interaction in GLS, *t*-test p = 0.01) and this difference increased as a function of yearday (significant difference in slopes, *t*-test p = 0.005).

Although the placement of the transducer on the saildrone is shallower than typical on most research vessels, measurements of backscatter and individual acoustic targets were restricted to > 4 m depth. We found no significant difference between day and night backscatter (*t*-test comparing day and night on all sampling days, p = 0.27), indicating that there were not a significant number of scatterers migrating above the sampling range during the surveys. Although it is possible that some scatterers remained shallower than the transducer at all times, it is unlikely that we missed a large portion of the fish population which would have had to remain above the insonified depth throughout the entire survey period.

Backscattering cross-section (σ_{bs}) measurements were obtained from 252,949 acoustic single targets detected during the four small-scale surveys. Daily mean σ_{bs} was positively related to yearday ($\sigma_{bs} = -7.68 \times 10^{-6} + 4.54 \times 10^{-8}$(yearday), $p < 0.001$, r^2 = 0.44; Fig. 6e), which results in a predicted increase in σ_{bs} from 1.7×10^{-6} (± 1.4×10^{-6} SE) to 3.5×10^{-6} (± 1.6×10^{-6} SE) between the midpoints of the first and fourth small-scale survey (Table 1). Estimates of standard length derived from σ_{bs} correspond to a change in length of 2.1 cm between the midpoints of the first and last survey (3.4–

Table 1. Summary of small-scale survey observations. The mean s_A, model-predicted backscattering cross-section (σ_{bs}) at the midpoint of each small-scale survey, abundance from 38-kHz backscatter, and estimated standard length of gadids are given. Standard errors are given in parentheses. Lengths were calculated from the model-predicted σ_{bs} at each survey midpoint using the TS–length relationship defined for Arctic cod (Geoffroy et al. 2016, Table S1).

	20 Jul–03 Aug	23 Jul–12 Aug	13–28 Aug	30 Aug–11 Sept
Mean s_A (m^2 nmi^{-2})	197 (± 53)	177 (± 76)	281 (± 79)	369 (± 80)
σ_{bs} (m^2)	1.7×10^{-6} (± 1.4×10^{-6})	2.0×10^{-6} (± 1.4×10^{-6})	2.8×10^{-6} (± 1.5×10^{-6})	3.5×10^{-6} (± 1.6×10^{-6})
Abundance index (fish m^{-2})	2.5 (± 0.6)	2.0 (± 0.8)	2.2 (± 0.6)	2.3 (± 0.5)
Estimated length (cm)	3.4 (1.1, 5.1)	3.7 (1.6, 5.4)	4.7 (2.7, 6.4)	5.5 (3.5, 7.2)

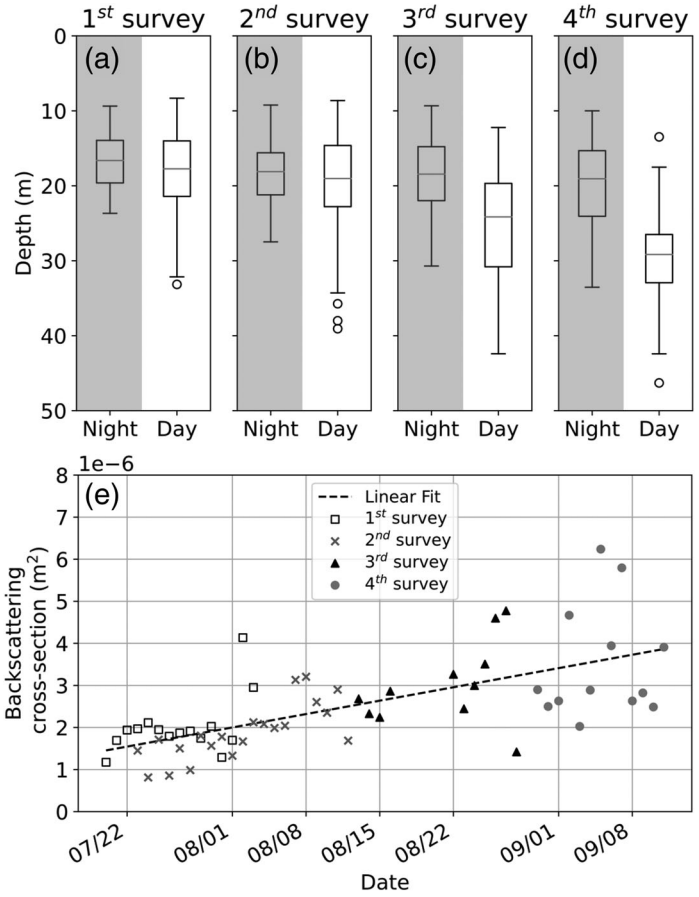

Fig. 6. (**a–d**) Distributions of nighttime and daytime hourly weighted mean depth of backscatter during the small-scale surveys. Boxes indicate the interquartile range, horizontal gray lines the median, vertical lines the 5% and 95% intervals. Circles indicate observations beyond the whiskers. (**e**) Daily means of backscattering cross-section (σ_{bs}) of all targets observed in small-scale surveys. Linear fit for the 53-d period is indicated by the black dashed line ($\sigma_{bs} = -7.68 \times 10^{-6} + 4.54 \times 10^{-8}$(yearday), $p < 0.001$, $r^2 = 0.44$).

5.5 cm). Using the model-predicted values of σ_{bs} from the first day and last day of the small-scale surveys (Fig. 6e), the change in length corresponds to a growth rate of 0.54 mm d^{-1} over the 53-d period (Table S1). This estimate of growth rate is sensitive to the specific TS–length relationship used to convert scattering strength to fish length, and the use of alternative relationships results in a large range of estimates (0.24–0.89 mm d^{-1}; Table S1).

Particle tracking

The passive particles in the simulation were primarily transported to the northeast (Figs. 7a-e, S2). By the end of the 60-d model run, the majority of particles were dispersed along the slope after being transported through Barrow Canyon (Fig. 7e). Initial movement of particles out of the survey region (Fig. 7a,b) was in two directions; particles in the northwest region of the survey area moved north toward Hanna Shoal, while the remainder of the particles followed the Alaska coastline to the northeast.

From 20 July to 02 August, particles were advected out of the small-scale survey region at a consistent rate, with the proportion remaining in the small-scale survey area decreasing from 49% to 33% (Fig. 7f). The rate of advection out of the small-scale survey region decreased from 02 August to 25 August, when the proportion of particles in the survey region increased to ~ 40% and there were periods where particles returned to the region from the north. Thereafter the rate of export increased, with only 11% of all particles remaining in the survey area by mid-September. Through most of the model run, the proportion of particles along the Beaufort/Chukchi slope steadily increased. By 18 September, or 60 d after the start of the first small-scale survey, 65% of particles had been advected seaward of the shelf break (> 100 m bottom depth) in the Chukchi and Beaufort Seas (Fig. 7e). The model runs produced similar results with particles tracked across depths of 10–40 m (Fig. 7f), indicating that (1) the system is strongly barotropic, that is, there is little vertical shear to the flow; and (2) inferences drawn from the model are not sensitive to fish depth.

Discussion

Acoustic surveys of age-0 gadids

Although the timing and location of spawning events are not known, large numbers of age-0 Arctic cod have been previously observed in the Chukchi Sea in the late summer and fall (De Robertis et al. 2017). The absence of a large population of age-1+ Arctic cod suggests that age-0 fish found in the eastern Chukchi Sea likely originated elsewhere, and that either overwinter mortality is high or they do not remain in place as they grow to maturity. This mortality and/or emigration is likely also occurring for other gadids including age-0 walleye pollock, for which large spawning stocks are observed in the Bering Sea but few age-1+ fish have been reported in the eastern Chukchi Sea (Goddard et al. 2014). We analyzed repeat acoustic surveys and used particle tracking simulations to gain insights into possible directions of arrival and movement of these age-0 gadids through the eastern Chukchi Sea, and whether the absence of older individuals is most likely due to mortality or emigration of age-0 individuals.

Although we were not able to directly sample acoustic targets, acoustic scatterers throughout the areas surveyed by the saildrones have spatial distributions and scattering properties that are consistent with those expected from age-0 gadids. Backscatter was highest in the northeastern Chukchi Sea, consistent with observations from previous surveys in which trawl samples in that area were dominated by large numbers of age-0 Arctic cod (Quast 1974; Eisner et al. 2013; De Robertis et al. 2017). The large-scale survey estimates of mean s_A (144 and 188 m^2 nm^{-2}) are similar in magnitude with estimates observed in previous acoustic surveys in the region

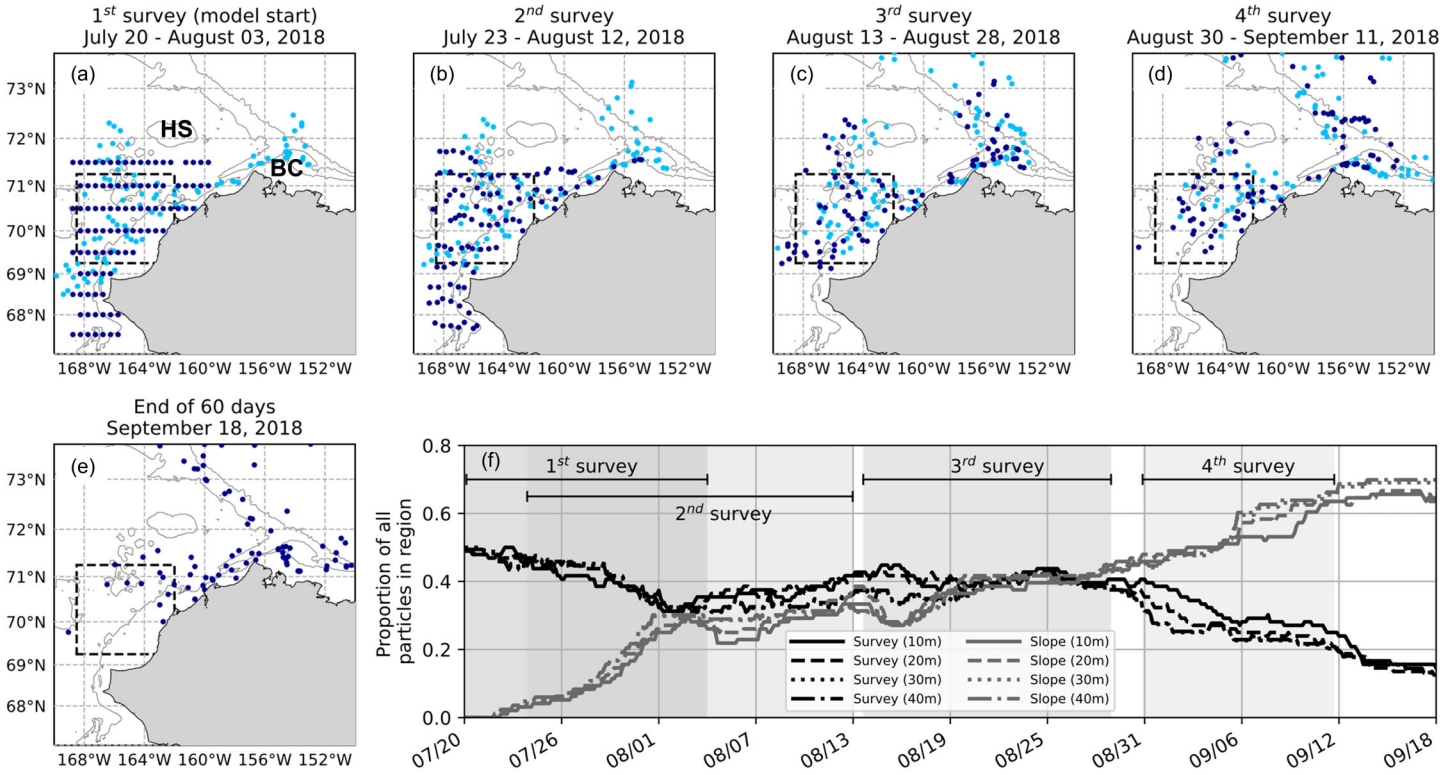

Fig. 7. Results of particle tracking model. (**a–d**) Locations of particles at 20 m depth at the start (dark blue circles) and end (light blue circles) of the (**a**) 1st, (**b**) 2nd, (**c**) 3rd, and (**d**) 4th small-scale surveys. Particles were seeded on 20 July at the center of each 0.5° grid cell of the first-large-scale survey (see Fig. S2). The locations of Hanna Shoal (HS) and Barrow Canyon (BC) are indicated in the first panel. (**e**) Locations of particles seeded at 20 m depth at the end of the 60-d model run. The area indicated by the dashed box represents the small-scale survey region. The 40-, 100-, and 1000-m depth contours are shown. (**f**) Proportion of particles remaining within the small-scale survey region (black lines), and particles transported to the Beaufort Sea and Beaufort/Chukchi slope (> 100 m bottom depth, gray lines) over a period of 2 months from the start of the 1st survey. Model results for particles seeded at fixed depths of 10–40 m are shown. The time periods of the four small-scale surveys are indicated by the gray shaded regions and lines. Note that the 1st and 2nd survey periods overlapped.

(63.6 and 164.9 m^2 nm^{-2} observed in 2012 and 2013), in which age-0 Arctic cod < 6 cm in length were the dominant contributors to 38-kHz backscatter (De Robertis et al. 2017). More recently, preliminary data from midwater trawl surveys in 2017 and 2019 indicate that primary scatterers across the shelf are age-0 gadids < 6 cm in length, and that while Arctic cod are the historically dominant scatterers, age-0 pollock may be becoming more abundant (R. M. Levine unpubl.). The σ_{bs} measurements observed in the four small-scale surveys (1.7×10^{-6} to 3.5×10^{-6} m^2, Table 1) are consistent with observed in situ observations of both age-0 Arctic cod and walleye pollock < 6 cm (Brodeur and Wilson 1996; Geoffroy et al. 2016) rather than the much higher σ_{bs} expected for larger individuals. For example, the σ_{bs} for a 15-cm Arctic cod is ~ 8-fold greater than for a 3.5-cm fish (Geoffroy et al. 2016), and ~ 14-fold greater for a 15-cm age-1 pollock than a 3.5-cm age-0 (Brodeur and Wilson 1996; Traynor 1996). Although estimates of length are sensitive to the choice of TS–length relationship (Table S1), the σ_{bs}-derived lengths are consistent with the length distributions of age-0 gadids observed in previously collected trawl samples in the region (mean length of 3.5 cm, 99.7% of fish < 6.5 cm in August–September reported in De Robertis et al. 2017). These multiple lines of indirect evidence support our assumption that age-0 gadids dominated contributions to backscatter in the saildrone surveys.

The repeat acoustic surveys indicate that, while the spatial distribution of fishes in the northeastern Chukchi Sea did not change significantly from late July to early September of 2018, acoustic backscatter increased by ~ 87% during this period. The observed increase in acoustic backscatter could have resulted from either an increase in the abundance of scatterers, changes in the composition (i.e., size) of the scatterers, or a combination of both. During the small-scale surveys, σ_{bs} between the midpoint of the first and fourth small-scale survey increased 104%. This suggests that the size distribution of fishes in the survey region may have shifted toward larger individuals. Over the same period, estimated fish density derived from the acoustic observations remained consistent

(2.0–2.5 fish m^{-2}, with overlapping standard errors, see Table 1). These estimated fish densities are similar to those observed in previous surveys (0.6 age-0 Arctic cod m^{-2} in 2012 and 2.2 Arctic cod m^{-2} in 2013, De Robertis et al. 2017).

Despite substantial variability, there is a unimodal distribution of σ_{bs} which increases over time, consistent with fish growth (Fig. S3). σ_{bs} is largely driven by swimbladder size, and although variability is high, average backscattering strength of individuals increases with length (Traynor 1996; Parker-Stetter et al. 2011). The changes in σ_{bs} corresponded to an estimated growth rate of 0.54 mm d^{-1} during the small-scale survey period. This growth rate is larger than measured rates from previous field and laboratory observations of age-0 Arctic cod (0.26 mm d^{-1} at 50 mm length, Hop et al. 1997; 0.19–0.24 mm d^{-1} Bouchard and Fortier 2011). However, growth rate is sensitive to the choice of TS–length relationship (0.24–0.89 mm d^{-1} depending on the relationship used, Table S1). Furthermore, σ_{bs} is orientation dependent (Foote 1980), and these estimates of growth assume consistent average orientation distributions over time. Although the uncertainties are large, the increase in σ_{bs} is likely related to growth, and it may ultimately be possible to estimate growth rates of Arctic gadids by measuring target strength in some circumstances. In future work, this uncertainty can be reduced by assessing TS–length relationships directly by coupling these observations with direct sampling of fish lengths.

The observed changes in vertical distribution (change in mean nighttime depth from 17.7 to 30.0 m during small-scale surveys) provide further evidence that growing age-0 gadids may have dominated the acoustic observations. As eggs and larvae, both Arctic cod and walleye pollock are predominantly surface associated (Spencer et al. 2020), drifting until their swimming ability develops and their swimbladder fills. Individuals exhibit an ontogenetic migration, descending deeper in the water column as they age. This transition in Arctic cod and walleye pollock occurs at a length of > 30 mm, when pelagic juveniles vertically shift to deeper water during daytime, typically observed in late summer (Brodeur et al. 2000; Ponomarenko 2000; Bouchard and Fortier 2011). In the saildrone surveys, diel vertical migration behavior was initiated when mean TS-derived lengths were > 30 mm. This behavior also coincided with the onset of night in late-July during both the first and second small-scale surveys. This change is consistent with expected behavior for gadids as individuals increase in size over time. Together, the observed σ_{bs} and increased vertical migration suggest that increasing backscatter may be due to individual growth.

Suitability of the Chukchi Sea as a nursery

Minimal changes were observed in the spatial distribution of fish during the survey period, which is inconsistent with a single, spatially restricted pulse of fish being advected across the Chukchi shelf. If there was a continuous northward transport, a single short spawning pulse from the south would result in a northward shift in the center of gravity of the population over time, and/or large changes in abundance between surveys. We hypothesized two alternative mechanisms to account for our observations: (1) a greatly extended spawning period that continues late into summer, with fish continuously transported north at a steady rate with balanced immigration and emigration; or, (2) retention of a population established by mid-July for most of the summer. The latter of these scenarios would be consistent with Arctic cod in other regions of the western Arctic where the majority of hatching occurs during a ~ 2-month period in late spring (Bouchard et al. 2016).

Age-0 fish populations may be enhanced by being be retained on the Chukchi shelf in summer to use the region as a nursery. Predation from piscivorous fish is likely low, as large fishes are scarce in the region (Sigler et al. 2011; De Robertis et al. 2017). Piscivorous seabirds are widely distributed and abundant throughout the Bering, Chukchi, and Beaufort Seas (Kuletz et al. 2015), and thus seabird predation pressure during open-water season is relatively consistent throughout the region. In summer, seabird foraging hotspots occur on the boundaries of the Chukchi shelf near Bering Strait and to the north along Barrow Canyon, where there is also a seasonal increase marine mammal presence (Kuletz et al. 2015).

Water temperatures on the Chukchi shelf are also likely to be more conducive for growth than conditions farther north (Laurel et al. 2016). Saildrone measurements of temperature and salinity were limited to the upper 0.5 m, thus it was not possible to directly assess the conditions at the same depths as the fish. However, backscatter was lowest in the northernmost areas of the large-scale survey area (Fig. 3), where low surface water temperatures and salinities suggested recent mixing with the meltwater which typically overlays cold winter water (Weingartner et al. 2013; Danielson et al. 2017). De Robertis et al. (2017) observed that Arctic cod on the Chukchi shelf were largely present at intermediate temperatures (3.4–6.6°C) and high salinities (> 30.4 psu) typical of Bering/Chukchi Summer Water. The Bering/Chukchi Summer Water flows north into the Chukchi Sea from the northern Bering Sea shelf (Coachman et al. 1975; Danielson et al. 2017) and gradually replaces the surface meltwater and deep winter water on the Chukchi shelf (Weingartner et al. 2013). The warmer Bering/Chukchi Summer Water is within the temperature range (2–8°C) observed for maximum growth in Arctic cod and positive growth potential in both walleye pollock and saffron cod (Laurel et al. 2016).

Advective influences on age-0 fishes

The low backscatter in areas near meltwater indicates that these fish are unlikely to be originating from the north or areas influenced by recent ice melt and are either passively or actively remaining in warmer conditions. The Chukchi shelf is a highly advective environment, where advection is likely to dominate over the directed swimming movements of small

fishes. The association of age-0 gadids with warmer water conditions supports the hypothesis that the age-0 gadids observed on the Chukchi shelf are likely advected northward from spawning areas to the south. Advective transport north across the Chukchi shelf is generally attributed to both local winds and a far field forcing relating to a sea level difference between the Pacific and the Arctic (see Woodgate et al. 2005 for discussion). Since 1990, the annual mean northward velocity of the flow through the Bering Strait has ranged from ~ 18 (± 2) cm s^{-1} in 2001 to ~ 28 (± 3) cm s^{-1} in 2014 (lowest and highest annual mean velocities of the 1991–2015 period; Woodgate 2018). This includes periods of southward flow and thus the northward mode speed is higher (from ~ 20 to > 40 cm s^{-1}, Woodgate 2018 their Fig. 4). In the northeastern Chukchi Sea, the mean velocities of the upper 10 m of the water column in summer average ~ 8 cm s^{-1}, ranging from 0.5 to 22.8 cm s^{-1} from 2010 to 2015 (Stabeno et al. 2018). In respiration experiments, maximum aerobic swim speeds of Arctic cod were 3 to 3.6 body lengths s^{-1} (12–14 cm s^{-1} for a 4-cm fish) during burst swimming activity (Kunz et al. 2018). In studies of related gadid species, routine swimming speeds of juvenile fish were 0.5 to 0.6 body lengths s^{-1} (2–2.4 cm s^{-1} for a 4-cm fish, Peck et al. 2006). For age-0 gadids of 3.5 cm length, this suggests a routine swimming speed of approximately 1.9 cm s^{-1}, which is an order of magnitude lower than typical advective currents. These estimates support the hypothesis that passive transport likely plays a dominant role determining the distribution of age-0 gadids on the Chukchi shelf, and that swimming behaviors have relatively small impacts on long-term distributions.

In late summer 2018, transport simulations suggest that age-0 gadids were advected northward, likely to the Beaufort and Chukchi slopes and Arctic basin. As expected, the model indicated that net transport was northward, with 90% of modeled particles released in the large-scale survey area dispersed along the shelf or slope to the north of the survey area at the end of the 60-d model run. However, during the month of August, only a few particles left the survey area, and during some periods transport reversed to increase particle abundance within the small-scale survey area (Figs. 7f, S2). The decrease in the rate of particles leaving the survey area and subsequent return of particles suggests that age-0 gadids are retained on the Chukchi shelf by episodic flow reversals. Estimates of retention based on particle transport from the survey area are consistent at 10, 20, 30, and 40 m depth (depths where the bulk of the backscatter occurred throughout the survey period). This suggests that variations in horizontal advection of fishes are likely insensitive to vertical movements or water column position.

Flow reversals similar to those occurring in the 2018 particle tracking model are commonly observed in the northeastern Chukchi Sea, and are associated with strong southward winds (Woodgate et al. 2005; Stabeno et al. 2018; Pisareva et al. 2019). De Robertis et al. (2017) speculated that difference in age-0 Arctic cod distribution between 2012 and 2013 may be linked to variability in currents and prey availability, and recent work has proposed variation in wind-driven retention as an explanation (Vestfals et al. 2019). Woodgate et al. (2005) developed a linear model for determining water velocity in the northeastern Chukchi Sea as a function of the pressure head forcing and surface wind speed. Offshore of Cape Lisburne, assuming a baseline pressure head velocity of 9.4 cm s^{-1} (see Table 3 in Woodgate et al. 2005), surface wind speed would need to exceed 7.2 m s^{-1} to the south to balance the pressure head forcing, temporarily stopping northward transport. Wind speed measurements from the saildrones indicate that from 01 August to 30 August, the mean velocity of the north–south wind component was 2.3 m s^{-1} to the south, with 21 days having mean southward winds (Fig. S4). However, during 10.3% of August, wind velocity to the south was > 7.2 m s^{-1}, during which predicted net northward transport would be near zero or negative. This simplistic calculation is supported by the particle tracking model which shows this wind reversal was sufficient to account for the particle retention on the shelf. We hypothesize that wind-driven relaxation in northward transport may be responsible for, and predict, retention of age-0 gadids in the northeastern Chukchi Sea.

It also seems reasonable to hypothesize that interannual variations in circulation influence advection and subsequent retention of age-0 gadids in the Chukchi Sea. Transport through the Bering Strait (which is generally indicative of the northward flux through the Chukchi Sea, Woodgate et al. 2005) estimated from near-bottom velocity data indicates that monthly mean transport during summer 2018 (R. A. Woodgate pers. comm.) was similar to the 1990–2004 climatology (Woodgate et al. 2005), even though in the annual mean, 2018 was higher in flow than the climatology. Thus, as it is summer that most concerns us, it is likely that the observed summer residence time of age-0 gadids in the Chukchi in 2018 is fairly typical, and suggests a hypothesis that cold-adapted species such as Arctic cod may have adapted to spawn at a time and place that more or less reliably places larvae in this apparent nursery area.

The Pacific Arctic is currently undergoing rapid changes, including increased northward transport through Bering Strait in recent decades (Woodgate 2018). These changes in advection, temperature, and ice cover have the potential to alter Arctic gadid populations. Bouchard et al. (2017) proposed that an initial decrease in ice cover, resulting in warmer conditions, would increase survival and growth of larval Arctic cod. However, continued temperature increases beyond their preferred growth range could depress physiological condition and survival of larval Arctic cod, while enhancing conditions for larval walleye pollock (Koenker et al. 2018). Winter spawning provides a lengthy growth period for Arctic cod, during which maximizing prewinter size may be important for survival (Bouchard and Fortier 2011). Increased northward transport in summer may more quickly transport Arctic cod off the shelf

and into the Arctic basin, shortening time available for growth in this potentially favorable nursery environment.

Increased input of Pacific water onto the shelf may also increase the presence of subarctic and boreal gadids, increasing competition and predation among pelagic species (Sigler et al. 2011). This transition has already been observed in the Barents Sea, where larger boreal species have expanded their distribution, increasing predation on and competition with smaller Arctic species (Fossheim et al. 2015). Subarctic gadids of high abundance in the Bering Sea such as walleye pollock and Pacific cod may be more likely to be transported north, following the same advective pathways across the Chukchi shelf as Arctic cod. Evidence from recent midwater surveys conducted in the region (R. M. Levine unpubl.) suggest other broadly distributed fishes such as walleye pollock or saffron cod have the potential to move further north, increasing in abundance on the Chukchi shelf as conditions warm (Huntington et al. 2020). The potential for these species to survive overwinter in the Arctic, however, is still unknown.

We found that distributions of age-0 gadids in the Chukchi Sea are strongly driven by two factors: advection and retention within specific water masses. Further studies are needed to better understand specific oceanographic features (e.g., currents, fronts, ice presence, water masses) and to investigate their demographic effects on gadids in the region. For example, in situ observations of fish movement and behavior (e.g., target tracking from moored acoustic instruments; Kaartvedt et al. 2009) paired with direct observations of currents have potential to better constrain potential pathways for transport of fishes, resolve the timing and seasonal dynamics of their development from eggs to juveniles, and predict recruitment into downstream populations along the Beaufort and Chukchi Sea slope.

Insights on Arctic fishes from USV observations

Traditionally, acoustic surveys have relied on trawl sampling of species and size composition to convert acoustic backscatter into abundance estimates (Simmonds and MacLennan 2005). Recent advances in the integration of echosounders into autonomous platforms have increased our ability to measure acoustic backscatter remotely over long periods (Greene et al. 2014; Mordy et al. 2017; Benoit-Bird et al. 2018; Ohman et al. 2019). We used the endurance of the saildrones to collect a large number of acoustic observations over an extended period of time which would have been prohibitively expensive and logistically difficult using ships. These repeat acoustic surveys spanning large spatial and temporal scales enabled us to constrain the movement of age-0 gadid fishes on the Chukchi shelf and made it possible to determine a TS and approximate a growth rate. These insights into the transport, growth, origins, and fate of the age-0 gadid population were made possible by the high spatial and temporal coverage offered by autonomous platforms.

However, with current technology, it remains challenging, in most cases, to validate species composition, size, sex, and other organismal properties by acoustic methods alone (Bassett et al. 2018). Thus, the key challenge going forward is not how to measure acoustic scattering from autonomous vehicles, but how best to use these measurements to understand the abundance, distribution, and behavior of marine organisms (De Robertis et al. 2019). While autonomous acoustic surveys cannot definitively identify the species and size composition of acoustic scatterers, they can be effective in regions where other data have shown that a single or distinguishable group of dominant scatterers enables interpretation of acoustic data (Mordy et al. 2017; De Robertis et al. 2019). Low-diversity, high-latitude regions may be favorable for autonomous echosounder measurements because backscatter is often dominated by a single species or group (Geoffroy et al. 2011; De Robertis et al. 2019).

With its low pelagic diversity, the Chukchi Sea provides a good ecosystem for the application of autonomous acoustic survey methods. However, Arctic ecosystems are undergoing changes that may alter species compositions (e.g.,Fossheim et al. 2015; Huntington et al. 2020), and the assumptions that make these inferences possible are likely to change with time. The increased presence of species with similar acoustic properties will limit the ability to address species-specific questions without additional sampling in rapidly changing ecosystems such as the Arctic, although inference at the community level (e.g., gadids) may be feasible. Future studies of high-latitude marine environments (e.g., Arctic, Antarctic) may benefit from the use of USVs and other autonomous platforms allowing for acoustic measurement of fish and macrozooplankton populations, with the potential to expand into more complex environments and applications as the methodologies for remote species identification improve.

Conclusions

Repeat saildrone surveys indicated that advection resulted in the retention of age-0 gadids on the Chukchi Sea shelf throughout the summer where they underwent in situ growth. These fish likely originated south of the central Chukchi Sea and were advected onto the northeast shelf. In late summer, transport simulations suggest that advection played a larger role than swimming and that these fishes were passively advected further north to the Beaufort and Chukchi slopes and Arctic basin. Variations in transport rate and trajectory may account for the interannual variability in the density and distribution of pelagic fishes on the Chukchi shelf. In a changing climate, changes in circulation and water column conditions may alter the future structure of pelagic communities in the Pacific Arctic and the suitability of the Chukchi shelf as a favorable nursery area. Although Arctic cod are currently the dominant gadid in the region, increasing temperatures and earlier transport off the Chukchi shelf could

limit age-0 growth prior to their first winter, and increased subarctic pelagic fishes such as walleye pollock may lead to increased predation pressure and competition that may further limit the Arctic cod population (Fossheim et al. 2015; Huntington et al. 2020). New technologies such as autonomous vehicles are likely to provide opportunities to better quantify perturbations of this rapidly changing ecosystem.

References

Bassett, C., A. De Robertis, and C. D. Wilson. 2018. Broadband echosounder measurements of the frequency response of fishes and euphausiids in the Gulf of Alaska. ICES J. Mar. Sci. **75**: 1131–1142. doi:10.1093/icesjms/fsx204

Benoit-Bird, K. J., T. Patrick Welch, C. M. Waluk, and others. 2018. Equipping an underwater glider with a new echosounder to explore ocean ecosystems. Limnol. Oceanogr. Methods **16**: 734–749. doi:10.1002/lom3.10278

Bouchard, C., and L. Fortier. 2011. Circum-arctic comparison of the hatching season of polar cod *Boreogadus saida*: A test of the freshwater winter refuge hypothesis. Prog. Oceanogr. **90**: 105–116. doi:10.1016/j.pocean.2011.02.008

Bouchard, C., S. Mollard, K. Suzuki, D. Robert, and L. Fortier. 2016. Contrasting the early life histories of sympatric Arctic gadids *Boreogadus saida* and *Arctogadus glacialis* in the Canadian Beaufort Sea. Polar Biol. **39**: 1005–1022. doi:10.1007/s00300-014-1617-4

Bouchard, C., M. Geoffroy, M. LeBlanc, A. Majewski, S. Gauthier, W. Walkusz, J. D. Reist, and L. Fortier. 2017. Climate warming enhances polar cod recruitment, at least transiently. Prog. Oceanogr. **156**: 121–129. doi:10.1016/j.pocean.2017.06.008

Bradstreet, M. S. W., K. J. Finley, A.-D. Sekerak, W. B. Griffiths, C. R. Evans, M. F. Fabijan, and H. E. Stallard. 1986. Aspects of the biology of Arctic Cod (*Boreogadus saida*) and its importance in Arctic marine food chains. Can. Tech. Rep. Fish. Aquat. Sci. Fish. Aquat. Sci. **1491**: 193.

Brodeur, R. D., and M. T. Wilson. 1996. Mesoscale acoustic patterns of juvenile walleye Pollock (*Theragra chalcogramma*) in the western Gulf of Alaska. Can. J. Fish. Aquat. Sci. **53**: 1951–1963. doi:10.1139/cjfas-53-9-1951

Brodeur, R. D., M. T. Wilson, and L. Ciannelli. 2000. Spatial and temporal variability in feeding and condition of age-0 walleye Pollock (*Theragra chalcogramma*) in frontal regions of the Bering Sea. ICES J. Mar. Sci. **57**: 256–264. doi:10.1006/jmsc.1999.0525

Coachman, L. K., K. Aagaard, and R. B. Tripp. 1975. Bering Strait: The regional physical oceanography. Univ. Washington Press, 172 p.

Corlett, W. B., and R. S. Pickart. 2017. The Chukchi slope current. Prog. Oceanogr. **153**: 50–65. doi:10.1016/j.pocean.2017.04.005

Danielson, S. L., L. Eisner, C. Ladd, C. Mordy, L. Sousa, and T. J. Weingartner. 2017. A comparison between late summer 2012 and 2013 water masses, macronutrients, and phytoplankton standing crops in the northern Bering and Chukchi seas. Deep-sea Res. Part II Top. Stud. Oceanogr. **135**: 7–26. doi:10.1016/j.dsr2.2016.05.024

De Robertis, A., K. Taylor, C. D. Wilson, and E. V. Farley. 2017. Abundance and distribution of Arctic cod (*Boreogadus saida*) and other pelagic fishes over the U.S. Continental Shelf of the Northern Bering and Chukchi seas. Deep-Sea Res. Part II Top Stud. Oceanogr. **135**: 51–65. doi:10.1016/j.dsr2.2016.03.002

De Robertis, A., N. Lawrence-Slavas, R. Jenkins, and others. 2019. Long-term measurements of fish backscatter from Saildrone unmanned surface vehicles and comparison with observations from a noise-reduced research vessel. ICES J. Mar. Sci **76**: 2459–2470. doi:10.1093/icesjms/fsz124

Demer, D.A. and others 2015. Calibration of acoustic instruments. ICES Coop. Res. Rep. No. 326. 133 p.

Eisner, L., N. Hillgruber, E. Martinson, and J. Maselko. 2013. Pelagic fish and zooplankton species assemblages in relation to water mass characteristics in the northern Bering and southeast Chukchi seas. Polar Biol. **36**: 87–113. doi:10.1007/s00300-012-1241-0

Ershova, E. A., R. R. Hopcroft, and K. N. Kosobokova. 2015. Inter-annual variability of summer mesozooplankton communities of the western Chukchi Sea: 2004–2012. Polar Biol. **38**: 1461–1481. doi:10.1007/s00300-015-1709-9

Foote, K. G. 1980. Effect of fish behaviour on echo energy: The need for measurements of orientation distributions. ICES J. Mar. Sci. **39**: 193–201. doi:10.1093/icesjms/39.2.193

Forster, C. E., B. L. Norcross, F. J. Mueter, E. A. Logerwell, and A. C. Seitz. 2020. Spatial patterns, environmental correlates, and potential seasonal migration triangle of polar cod (*Boreogadus saida*) distribution in the Chukchi and Beaufort seas. Polar Biol. **43**: 1073–1094. doi:10.1007/s00300-020-02631-4

Fossheim, M., R. Primicerio, E. Johannesen, R. B. Ingvaldsen, M. M. Aschan, and A. V. Dolgov. 2015. Recent warming leads to a rapid borealization of fish communities in the Arctic. Nat. Clim. Change **5**: 673–677. doi:10.1038/nclimate2647

Frey, K. E., G. W. K. Moore, L. W. Cooper, and J. M. Grebmeier. 2015. Divergent patterns of recent sea ice cover across the Bering, Chukchi, and Beaufort seas of the Pacific Arctic region. Prog. Oceanogr. **136**: 32–49. doi:10.1016/j.pocean.2015.05.009

Geoffroy, M., D. Robert, G. Darnis, and L. Fortier. 2011. The aggregation of polar cod (*Boreogadus saida*) in the deep Atlantic layer of ice-covered Amundsen Gulf (Beaufort Sea) in winter. Polar Biol. **34**: 1959–1971. doi:10.1007/s00300-011-1019-9

Geoffroy, M., A. Majewski, M. LeBlanc, S. Gauthier, W. Walkusz, J. D. Reist, and L. Fortier. 2016. Vertical

segregation of age-0 and age-1+ polar cod (*Boreogadus saida*) over the annual cycle in the Canadian Beaufort Sea. Polar Biol. **39**: 1023–1037. doi:10.1007/s00300-015-1811-z

Gjøsæter, H. 1995. Pelagic fish and the ecological impact of the modern fishing industry in the Barents Sea. Arctic **48**: 267–278. doi:10.14430/arctic1248

Goddard, P., R. Lauth, and C. Armistead. 2014. Results of the 2012 Chukchi Sea bottom trawl survey of Bottomfishes, crabs, and other Demersal macrofauna. U.S. Dep. Commer., NOAA Tech. Memo. NMFS-AFSC-278. 110 p.

Greene, C., and others. 2014. A wave glider approach to fisheries acoustics: Transforming how we monitor the Nation's Commercial Fisheries in the 21st century. Oceanography **27**: 168–174. doi:10.5670/oceanog.2014.82

Hinckley, S. 1987. The reproductive biology of walleye Pollock, *Theragra chalcogramma*, in the Bering Sea, with reference to spawning stock structure. Fish. Bull. **85**: 481–498.

Hogan, T. F., and others. 2014. The navy global environmental model. Oceanography **27**: 116–125. doi:10.5670/oceanog.2014.73

Hop, H., W. M. Tonn, and H. E. Welch. 1997. Bioenergetics of Arctic cod (*Boreogadus saida*) at low temperatures. Can. J. Fish. Aquat. Sci. **54**: 1772–1784. doi:10.1139/cjfas-54-8-1772

Horne, J. K. 2000. Acoustic approaches to remote species identification: A review. Fish. Oceanogr. **9**: 356–371. doi:10.1046/j.1365-2419.2000.00143.x

Huntington, H. P., and others. 2020. Evidence suggests potential transformation of the Pacific Arctic ecosystem is underway. Nat. Clim. Change. **10**: 342–348. doi:10.1038/s41558-020-0695-2

Kaartvedt, S., A. Røstad, T. A. Klevjer, and A. Staby. 2009. Use of bottom-mounted echo sounders in exploring behavior of mesopelagic fishes. Mar. Ecol. Prog. Ser. **395**: 109–118. doi:10.3354/meps08174

Koenker, B. L., L. A. Copeman, and B. J. Laurel. 2018. Impacts of temperature and food availability on the condition of larval Arctic cod (*Boreogadus saida*) and walleye Pollock (*Gadus chalcogrammus*). ICES J. Mar. Sci. **75**: 2370–2385. doi:10.1093/icesjms/fsy052

Kono, Y., H. Sasaki, Y. Kurihara, A. Fujiwara, J. Yamamoto, and Y. Sakurai. 2016. Distribution pattern of Polar cod (*Boreogadus saida*) larvae and larval fish assemblages in relation to oceanographic parameters in the Northern Bering Sea and Chukchi Sea. Polar Biol. **39**: 1039–1048. doi:10.1007/s00300-016-1961-7

Kuletz, K. J., M. C. Ferguson, B. Hurley, A. E. Gall, E. A. Labunski, and T. C. Morgan. 2015. Seasonal spatial patterns in seabird and marine mammal distribution in the eastern Chukchi and western Beaufort seas: Identifying biologically important pelagic areas. Prog. Oceanogr. **136**: 175–200. doi:10.1016/j.pocean.2015.05.012

Kunz, K. L., G. Claireaux, H.-O. Pörtner, R. Knust, and F. C. Mark. 2018. Aerobic capacities and swimming performance of polar cod (*Boreogadus saida*) under ocean acidification and warming conditions. J. Exp. Biol. **221**: jeb184473. doi:10.1242/jeb.184473

Lange, M., and E. Van Sebille. 2017. Parcels v0.9: Prototyping a Lagrangian Ocean analysis framework for the petascale age. Geosci. Model Dev. **10**: 4175–4186. doi:10.5194/gmd-10-4175-2017

Laurel, B. J., M. Spencer, P. Iseri, and L. A. Copeman. 2016. Temperature-dependent growth and behavior of juvenile Arctic cod (*Boreogadus saida*) and co-occurring North Pacific gadids. Polar Biol. **39**: 1127–1135. doi:10.1007/s00300-015-1761-5

Laurel, B. J., L. A. Copeman, M. Spencer, and P. Iseri. 2018. Comparative effects of temperature on rates of development and survival of eggs and yolk-sac larvae of Arctic cod (*Boreogadus saida*) and walleye Pollock (*Gadus chalcogrammus*). ICES J. Mar. Sci. **75**: 2403–2412. doi:10.1093/icesjms/fsy042

Logerwell, E., and others. 2015. Fish communities across a spectrum of habitats in the western Beaufort Sea and Chukchi Sea. Prog. Oceanogr. **136**: 115–132. doi:10.1016/j.pocean.2015.05.013

MacLennan, D. N., P. G. Fernandes, and J. Dalen. 2002. A consistent approach to definitions and symbols in fisheries acoustics. ICES J. Mar. Sci. **59**: 365–369. doi:10.1006/jmsc.2001.1158

Marsh, J. M., F. J. Mueter, and T. J. Quinn. 2019. Environmental and biological influences on the distribution and population dynamics of polar cod (*Boreogadus saida*) in the US Chukchi Sea. Polar Biol. **43**: 1055–1072. doi:10.1007/s00300-019-02561-w

Matley, J. K., A. T. Fisk, and T. A. Dick. 2012. Seabird predation on Arctic cod during summer in the Canadian Arctic. Mar. Ecol. Prog. Ser. **450**: 219–228. doi:10.3354/meps09561

Mecklenburg, C. W., and others. 2018. Marine fishes of the Arctic Region Volume II. CAFF Monitoring Series Report 28. Akureyri, Iceland: Conservation of Arctic Flora and Fauna.

Mordy, C., and others. 2017. Advances in ecosystem research: Saildrone surveys of oceanography, fish, and marine mammals in the Bering Sea. Oceanography **30**: 113–115. doi:10.5670/oceanog.2017.230

Norcross, B. L., B. A. Holladay, M. S. Busby, and K. L. Mier. 2010. Demersal and larval fish assemblages in the Chukchi Sea. Deep-Sea Res. Part II Top. Stud. Oceanogr. **57**: 57–70. doi:10.1016/j.dsr2.2009.08.006

Ohman, M. D., R. E. Davis, J. T. Sherman, K. R. Grindley, B. M. Whitmore, C. F. Nickels, and J. S. Ellen. 2019. Zooglider: An autonomous vehicle for optical and acoustic sensing of zooplankton. Limnol. Oceanogr. Methods **17**: 69–86. doi:10.1002/lom3.10301

Parker-Stetter, S. L., J. K. Horne, and T. J. Weingartner. 2011. Distribution of polar cod and age-0 fish in the U.S. Beaufort

Sea. Polar Biol. **34**: 1543–1557. doi:10.1007/s00300-011-1014-1

Peck, M. A., L. J. Buckley, and D. A. Bengtson. 2006. Effects of temperature and body size on the swimming speed of larval and juvenile Atlantic cod (*Gadus morhua*): Implications for individual-based modelling. Environ. Biol. Fishes **75**: 419–429. doi:10.1007/s10641-006-0031-3

Pinchuk, A. I., and L. B. Eisner. 2017. Spatial heterogeneity in zooplankton summer distribution in the eastern Chukchi Sea in 2012–2013 as a result of large-scale interactions of water masses. Deep-Sea Res. Part II Top. Stud. Oceanogr. **135**: 27–39. doi:10.1016/j.dsr2.2016.11.003

Pinheiro, J., D. Bates, S. DebRoy, D. Sarkar, and R Core Team. 2019. {nlme}: Linear and Nonlinear Mixed Effects Models. Available from https://cran.r-project.org/package=nlme

Pisareva, M. N., R. S. Pickart, P. Lin, P. S. Fratantoni, and T. J. Weingartner. 2019. On the nature of wind-forced upwelling in Barrow Canyon. Deep-Sea Res. Part II Top. Stud. Oceanogr. **162**: 63–78. doi:10.1016/j.dsr2.2019.02.002

Ponomarenko, V. 1968. Some data on the distribution and migrations of polar cod in the seas of the Soviet Arctic. Rapp. Procès Verbaux Réunions CIEM **158**: 131–135.

Ponomarenko, V. 2000. Eggs, larvae, and juveniles of polar cod *Boreogadus saida* in the Barents, Kara, and White Seas. J. Ichthyol. **40**: 165–173.

Quast, J. C. 1974. Density distribution of juvenile Arctic cod, *Boreogadus saida*, in the eastern Chukchi Sea in the fall of 1970. Fish. Bull., U.S **72**: 1094–1105.

Sawada, K., M. Furusawa, and N. J. Williamson. 1993. Conditions for the precise measurement of fish target strength in situ. J. Mar. Acoust. Soc. Jpn. **20**: 73–79. doi:10.3135/jmasj.20.73

Sigler, M., M. Renner, S. Danielson, L. Eisner, R. Lauth, K. Kuletz, E. Logerwell, and G. Hunt. 2011. Fluxes, fins, and feathers: Relationships among the Bering, Chukchi, and Beaufort seas in a time of climate change. Oceanography **24**: 250–265. doi:10.5670/oceanog.2011.77

Sigler, M. F., and others. 2017. Late summer zoogeography of the northern Bering and Chukchi seas. Deep-Sea Res. Part II Top Stud. Oceanogr. **135**: 168–189. doi:10.1016/j.dsr2.2016.03.005

Simmonds, J., and D. MacLennan. 2005. Fisheries acoustics: Theory and practice, 2nd ed. Blackwell.

Spear, A., J. Duffy-Anderson, D. Kimmel, J. Napp, J. Randall, and P. Stabeno. 2019. Physical and biological drivers of zooplankton communities in the Chukchi Sea. Polar Biol. **42**: 1107–1124. doi:10.1007/s00300-019-02498-0

Spencer, M. L., C. D. Vestfals, F. J. Mueter, and B. J. Laurel. 2020. Ontogenetic changes in the buoyancy and salinity tolerance of eggs and larvae of polar cod (*Boreogadus saida*) and other gadids. Polar Biol. **43**: 1141–1158. doi:10.1007/s00300-020-02620-7

Stabeno, P., N. Kachel, C. Ladd, and R. Woodgate. 2018. Flow patterns in the eastern Chukchi Sea: 2010–2015. J. Geophys. Res. Ocean. **123**: 1177–1195. doi:10.1002/2017JC013135

Steele, M., W. Ermold, and J. Zhang. 2008. Arctic Ocean surface warming trends over the past 100 years. Geophys. Res. Lett. **35**: 1–6. doi:10.1029/2007GL031651

Stevenson, D. E., and R. R. Lauth. 2019. Bottom trawl surveys in the northern Bering Sea indicate recent shifts in the distribution of marine species. Polar Biol. **42**: 407–421. doi:10.1007/s00300-018-2431-1

Traynor, J. 1996. Target-strength measurements of walleye Pollock (*Theragra chalcogramma*) and Pacific whiting (*Merluccius productus*). ICES J. Mar. Sci. **53**: 253–258. doi:10.1006/jmsc.1996.0031

Vestfals, C. D., F. J. Mueter, J. T. Duffy-Anderson, M. S. Busby, and A. De Robertis. 2019. Spatio-temporal distribution of polar cod (*Boreogadus saida*) and saffron cod (*Eleginus gracilis*) early life stages in the Pacific Arctic. Polar Biol. **42**: 969–990. doi:10.1007/s00300-019-02494-4

Wackernagel, H. 2013. Multivariate geostatistics: An introduction with applications. Springer Science & Business Media.

Weingartner, T., E. Dobbins, S. Danielson, P. Winsor, R. Potter, and H. Statscewich. 2013. Hydrographic variability over the northeastern Chukchi Sea shelf in summer-fall 2008–2010. Cont. Shelf Res. **67**: 5–22. doi:10.1016/j.csr.2013.03.012

Whitehouse, G. A., and K. Y. Aydin. 2016. Trophic structure of the eastern Chukchi Sea: An updated mass balance food web model. U.S. Dep. Commer., NOAA Tech. Memo. NMFS-AFSC-318. 175 p.

Woillez, M., J. C. Poulard, J. Rivoirard, P. Petitgas, and N. Bez. 2007. Indices for capturing spatial patterns and their evolution in time, with application to European hake (*Merluccius merluccius*) in the Bay of Biscay. ICES J. Mar. Sci. **64**: 537–550. doi:10.1093/icesjms/fsm025

Woodgate, R. A. 2018. Increases in the Pacific inflow to the Arctic from 1990 to 2015, and insights into seasonal trends and driving mechanisms from year-round Bering Strait mooring data. Prog. Oceanogr. **160**: 124–154. doi:10.1016/j.pocean.2017.12.007

Woodgate, R. A., K. Aagaard, and T. J. Weingartner. 2005. A year in the physical oceanography of the Chukchi Sea: Moored measurements from autumn 1990-1991. Deep-Sea Res. Part II Top. Stud. Oceanogr. **52**: 3116–3149. doi:10.1016/j.dsr2.2005.10.016

Acknowledgments

This work was funded by the North Pacific Research Board Arctic Research Program, NOAA's Pacific Marine Environmental Laboratory's Innovative Technology for Arctic Exploration program, NOAA's Alaska Fisheries Science Center, and the Joint Institute for the Study of the Atmosphere and Ocean (JISAO) under NOAA Cooperative Agreement NA15OAR4320063. The saildrone deployments would not have been possible without the contributions of Richard Jenkins and Dave Peacock (Saildrone, Inc.), and Ivar Wagnen (Kongsberg Simrad). We would also

like to thank the Alaska Waterways Safety Committee, Alaska Eskimo Whaling Commission, The North Slope Borough, and members of The Village of Wainwright, AK for their advice and assistance with saildrone operations. We thank the anonymous reviewers for their suggestions which improved this manuscript. This is contribution No. 5091 for Pacific Marine Environmental Laboratory, contribution No. 2020-1063 for JISAO, and contribution No. EcoFOCI-0947 for NOAA's Ecosystem Fisheries Oceanography Coordinated Investigations. Bering Strait mooring observations are funded by NSF-OPP (1304052 and 1758565) with data available from http://psc.apl.washington.edu/BeringStrait.html. Any use of trade, firm, or product names is for descriptive purposes only and does not imply endorsement U.S. Government. Findings of this paper do not necessarily represent the views of the National Oceanic and Atmospheric Administration.

Conflict of interest

None declared.

Submitted 14 May 2020
Revised 30 October 2020
Accepted 08 November 2020

Associate editor: Kelly Benoit-Bird